Computations and Parameterizations of the Nonlinear Energy Transfer in a Gravity-Wave Spectrum. Part II: Parameterizations of the Nonlinear Energy Transfer for Application in Wave Models

S. HASSELMANN AND K. HASSELMANN

Max-Planck Institut für Meteorologie, Hamburg, Federal Republic of Germany

J. H. ALLENDER

Chevron Oil Field Research Company, La Habra, CA 90631

T. P. BARNETT

Scripps Institution of Oceanography, La Jolla, CA 92093

(Manuscript received 17 September 1984, in final form 30 April 1985)

ABSTRACT

Four different parameterizations of the nonlinear energy transfer S_{nl} in a surface wave spectrum are investigated. Two parameterizations are based on a relatively small number of parameters and are useful primarily for application in parametrical or hybrid wave models. In the first parameterization, shape-distortion parameters are introduced to relate the distributions S_{nl} for different values of the peak-enhancement parameter γ. The second parameterization is based on an EOF expansion of a set of S_{nl} computed for a number of different spectral distributions. The remaining two parameterizations represent operator forms that contain the same number of free parameters as used to describe the wave spectrum. Such parameterizations with a matched number of input and output parameters are required for numerical stability in high-resolution discrete spectral models. A cubic, fourth-order diffusion-operator expression derived by a local-interaction expansion is found to be useful for understanding many of the properties of S_{nl}, but is regarded as too inaccurate in detail for application in most wave models. The best results are achieved with a discrete-interaction operator parameterization, in which a single interaction configuration, together with its mirror image (representing a two-dimensional continuum of interactions with respect to a variable reference wavenumber scale and direction) is used to simulate the net effect of the full five-dimensional interaction continuum.

1. Introduction

A traditional difficulty of numerical wave models has been the adequate representation of the source function S_{nl} describing the nonlinear energy transfer. Since the time needed to compute the exact source function expression greatly exceeds the practical limits set by an operational wave model, some form of parameterization is needed. In the original approach used by Barnett (1968) and Ewing (1971) the nonlinear transfer for any given spectrum was simply replaced by the transfer computed for an equivalently scaled reference spectrum of prescribed (Pierson-Moskowitz) shape. After the important role of the nonlinear transfer in controlling the shape and rate of evolution of a wind-sea spectrum was more clearly recognized (Mitsuyasu, 1968, 1969; Hasselmann *et al.*, 1973), it became apparent that more general parameterizations were needed which allowed for the influence of the spectral shape on the strength and distribution of the nonlinear transfer. Present second-generation wave models therefore normally include some form of shape sensitivity in the parameterization schemes for S_{nl}.

Nevertheless, a recent intercomparison study of wave models (Sea Wave Modeling Project—SWAMP; cf. The SWAMP Group, 1985) revealed that all present second-generation models exhibit similar, basic deficencies in their treatment of the nonlinear transfer. These may be attributed to two factors: first, the parameterization schemes used in present second generation models contain too few degrees of freedom to reproduce adequately the nonlinear transfer for an arbitrary spectral shape; and second, the dependence of the nonlinear transfer on spectral shape has simply not been sufficiently well explored through exact computations for the wide variety of wind-sea and mixed wind-sea/swell spectra which may be encountered in strongly varying wind fields, or in decaying wind situations in which the wind-sea is transformed into swell.

The first shortcoming is not just a question of the fidelity of the parameterization. More seriously, it leads to numerical instabilities in high-resolution, discrete

spectral models (cf. The SWAMP Group, 1985). This is overcome in practice by reducing the effective number of degrees of freedom used in the description of the spectrum to match the number of degrees of freedom used in the parameterization of the nonlinear transfer. However, this in effect reduces a discrete spectral model to a hybrid model. The solution to this difficulty is clearly to develop alternative, operator parameterizations of the nonlinear transfer in which the nonlinear source functions contain the same number of degrees of freedom as the spectrum itself.

To overcome the second deficiency, extensive computations of the exact nonlinear transfer expression are required for a wide variety of spectra. This has now become feasible through the development of a more efficient computation technique, described in Part I of this paper (Hasselmann and Hasselmann, 1985, referred to in the following as I), which exploits the symmetry of the wave–wave interactions. The ability to perform fast computations of the exact nonlinear transfer expression has a further important advantage in the present context. It is found in practice that parameterizations can be tested reliably only by actually incorporating them in a wave model and verifying that the wave growth simulated by the model agrees in standard test cases with the growth curves obtained with the same model using exact computations of the nonlinear transfer. Such integrations require repeated exact nonlinear transfer computations using an efficient integration technique.

We investigate various alternative parameterization methods. The simplest approach is a straightforward extension of the technique originally used by Barnett (1968) and Ewing (1971). The exact nonlinear transfer is first computed for a selected class of spectra characterized by relatively few spectral-shape parameters. In the wave model, the nonlinear transfer for a given spectrum is then simply replaced by the stored, previously computed exact transfer for an appropriate member of the selected spectral class whose shape most resembles the given model spectrum (the dependence on the spectral scale parameters is determined by theory). Two such parameterizations are developed (Sections 2 and 3). These parameterizations are useful for summarizing the general properties of the exact nonlinear transfer expression, but incorporate only a small number of degrees of freedom. They therefore cannot be reliably applied for spectral distributions that fall outside the limited family of spectra spanned by the chosen parameter space. They are nevertheless appropriate for hybrid models in which the spectral shape is restricted *a priori* in the model. However, if applied in high-resolution discrete spectral models, they not only do injustice to the basic flexibility of the spectral description, but actually lead to the aforementioned instabilities.

We accordingly consider two further parameterizations in which the nonlinear transfer is approximated by general nonlinear operator expressions.

In the first operator parameterization, the transfer integral is represented in the local-interaction approximation as a fourth-order, cubic diffusion operator (Section 4). Although this operator captures most of the basic features of the exact expressions and is useful for understanding the role of the nonlinear transfer in the spectral energy balance, it is not considered sufficiently accurate for quantitative calculations in most numerical wave models. In this respect the local-interaction approximation is comparable with the alternative expansions for narrowly peaked spectra developed by Longuet-Higgins (1976), Fox (1976), and Dungey and Hui (1979), which are also based on local-interaction approximations. (The narrow-peak approximation is not considered as a candidate operator parameterization here, however, as it contains too few degrees of freedom to be applied in a discrete wave model without spectral-shape constraints.)

An alternative nonlinear operator approximation is therefore developed that extends over a broader wavenumber interaction range (Section 5). The parameterization essentially mirrors the structure of the exact integral, but restricts the interactions to a discrete subset. Each wavenumber of the spectrum is allowed to interact with other components of the spectrum through only a small number of basic interaction configurations. In this manner the complete Boltzmann interaction integral over the full 5d-interaction phase space is reduced to a 2d-integral over a reference wavenumber, which defines the scale and orientation of the discrete interaction quadruplets. This brings the computation of the nonlinear source function to the same dimensional level as the remaining source functions. Experiments with a number of different interaction configurations finally led to the choice of two mirror-image quadruplets which yielded acceptable approximations to the exact transfer expression for a wide variety of spectra and reproduced both the basic fetch-limited spectral growth relations obtained with the exact nonlinear transfer expression and the response to a turning wind.

We regard this last parameterization as the most suitable form for incorporation in discrete wave models. It can readily be upgraded by including additional interaction configurations. However, as summarized in the concluding Section 6, the alternative parameterizations considered in this paper also have various merits: in illustrating the principal properties of the nonlinear transfer, in interpreting the response of a growing wind-sea spectrum to the driving source functions, or for application in parametrical or hybrid wave models containing fewer degrees of freedom than a fully resolving discrete spectral model.

2. Parameterization of the nonlinear transfer in terms of the peak-enhancement parameter γ

The principal dependence of the nonlinear transfer S_{nl} on the shape of a wind-sea spectrum can be de-

scribed in terms of the peak-enhancement parameter γ. This is defined for a wind-sea spectrum as the ratio of the level of the one-dimensional frequency spectrum at the peak frequency to the value of the equivalent Pierson-Moskowitz (PM) spectrum at the same peak frequency, the PM spectrum being adjusted to the same level at high frequencies (i.e., to the same value of Phillips' constant α).

The dependence of S_{nl} on γ explains the self-stabilization of the spectral shape, the shift of the peak to lower frequencies during the growth stage, and the energy transfer into the peak instead of the forward face of the spectrum for a fully developed Pierson-Moskowitz spectrum. (A summary of the principal properties of the nonlinear transfer is given in I, Section 3; cf. also Hasselmann and Hasselmann, 1981, Part II, Figs. 7–15. The transfer integral itself is discussed in I, Section 2.)

One could readily extend the original shape-independent parameterization of Barnett (1968) and Ewing (1971) to include an additional dependence on γ. However, the following parameterization scheme was found to be simpler. The nonlinear transfer functions for all wind-sea spectra are related to a standard reference spectrum

$$F(f, \varphi) = E(f)S(f, \varphi) \tag{2.1}$$

in which the one-dimensional spectrum is given by the mean JONSWAP spectrum

$$E(f) = \alpha g^2(2\pi)^{-4}f^{-5}\exp\left\{-\frac{5}{4}(f/f_m)^4\right\} \times \exp\left\{\ln\gamma\exp\left[-\frac{(f-f_m)^2}{2\sigma^2 f_m{}^2}\right]\right\} \tag{2.2}$$

with

$$\begin{aligned} \gamma &= 3.3 \\ \sigma &= \sigma_a = 0.07 \quad \text{for} \quad f < f_m \\ \sigma &= \sigma_b = 0.09 \quad \text{for} \quad f > f_m \end{aligned} \tag{2.3}$$

(cf. Hasselmann *et al.*, 1973) and the spreading function is of the Mitsuyasu-Hasselmann form

$$S(f, \varphi) = I(p)\cos^{2p}(\varphi/2) \tag{2.4}$$

with

$$p = 10^{0.99}(f/f_m)^\beta,$$

$$\beta = \begin{cases} 4.06 & \text{for} \quad f < f_m \\ -2.34 & \text{for} \quad f \geqslant f_m. \end{cases} \tag{2.5}$$

The normalization factor is given by $I(p) = 2^{(2p-1)}\pi^{-1}\cdot\Gamma^2(p+1)/\Gamma(2p+1)$ (Mitsuyasu *et al.*, 1975; Hasselmann *et al.*, 1980).

For a wind-sea spectrum for which $\gamma \neq \gamma_{\text{ref}} = 3.3$, the nonlinear transfer S_{nl} is found to be distorted relative to the nonlinear transfer for the reference spectrum. The distortion can be expressed sufficiently accurately for a spectrum of the general form (2.2) through a linear transformation of the frequency axis

$$(\nu - \nu_0) = B(\nu' - \nu_0') \tag{2.6}$$

and a scale factor A in the form

$$S'_{nl}(\nu', \varphi) = AS_{nl}(\nu, \varphi). \tag{2.7}$$

Here $S_{nl}(\nu, \varphi)$, $S'_{nl}(\nu', \varphi)$ denote the nonlinear transfer of the reference JONSWAP spectrum and the wind-sea spectrum (with $\gamma \neq 3.3$), respectively, $\nu = f/f_m$ is the normalized frequency of the reference JONSWAP spectrum, $\nu' = f'/f'_m$ the corresponding normalized frequency of the wind-sea spectrum, and ν_0 (=1.01), ν_0' denote the zero-crossing transition frequencies between the low-frequency positive lobe and the negative lobe of the one-dimensional transfer functions for the reference spectrum and wind-sea spectrum, respectively (cf. Fig. 1). The angular arguments in (2.7) are the same: it was found that no distortion of the angular distribution was required to achieve good agreement of the two-dimensional distributions of S_{nl} for different γ-values, provided the wind-sea and reference spectrum had the same spreading functions.

The three free parameters ν_0', A and B of the transformations obtained by best fitting the exact computation to the transformed reference case are plotted as functions of γ in Fig. 2. A comparison of the true (one-dimensional) nonlinear transfer and the parameterized transfer is shown in Fig. 3 for the γ-values 1, 2, 5. The agreement is reasonable, except in the second positive lobe at high frequencies. The discrepancy at higher frequencies could have been reduced by including a quadratic term in the frequency transformation (2.6). This was not done, however, as the precise form of the nonlinear source function at higher frequencies is irrelevant for most hybrid-type wave models for which this parameterization is most useful.

The dependence of ν_0', A and B on γ in Fig. 2 sum-

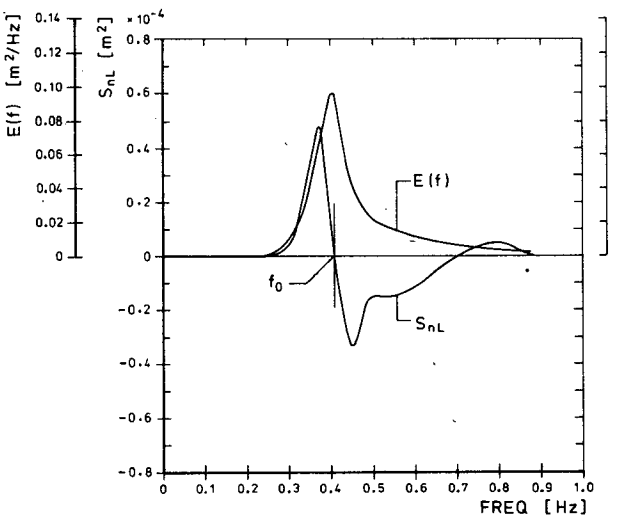

FIG. 1. One-dimensional spectrum and nonlinear transfer for a JONSWAP spectrum with spreading function (4.4).

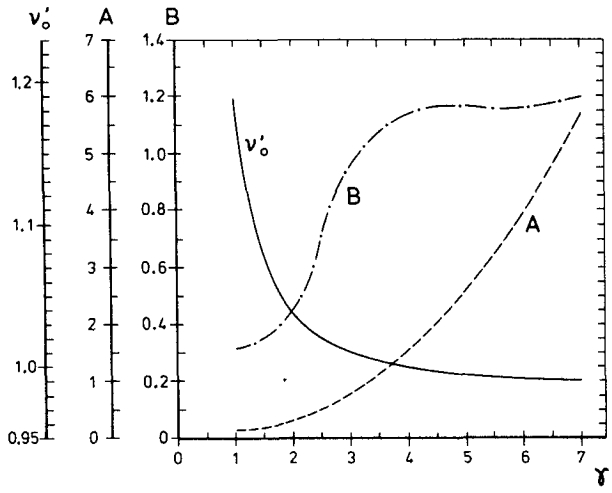

FIG. 2. Dependence of the three coefficients determining the transformations (4.6), (4.7) on γ.

marizes rather concisely the principal effects of the spectral shape on the nonlinear transfer (cf. I, Section 3): as γ approaches the fully developed value 1, the nonlinear transfer distribution shifts to higher frequencies (increasing ν_0'), the lobes become broader (decreasing B) and weaker (decreasing A). Note the two-order of magnitude decrease of the strength scale factor A as γ decreases from 7 to 1.

A parameterization of S_{nl} in terms of the single shape parameter γ is useful for modeling the transition of a wind-sea spectrum from a fetch-limited to a fully developed spectrum under normal growth conditions in which the spectrum has time to adjust locally to a quasi-equilibrium form, i.e., for conditions appropriate for a hybrid wave model. However, the parameterization cannot be introduced without further restraints directly into a fully resolving discrete spectral wave model, as the mismatch in the large number of degrees of freedom of the spectrum (typically several hundred) and the single free parameter of the nonlinear transfer leads to instabilities (cf. Section 4 and The SWAMP Group, 1985).

For application in a hybrid wave model, the form (2.7) needs to be projected on to the parameter space of the wave model. A more general parameterization of S_{nl} in terms of the shape parameters suitable for use in hybrid models is given by Hasselmann and Hasselmann (1981). In this method, the computed transfer functions S_{nl} for different values of the five JONSWAP parameters $\alpha, f_m, \gamma, \sigma_a, \sigma_b$ are projected directly on to the JONSWAP parameter space, yielding rates of change of the JONSWAP parameters as a function of the parameters themselves. The results are approximated by a linear matrix relation.

3. Parameterization of S_{nl} in terms of an EOF representation

An alternative method of describing the results of an ensemble of exact nonlinear transfer computations

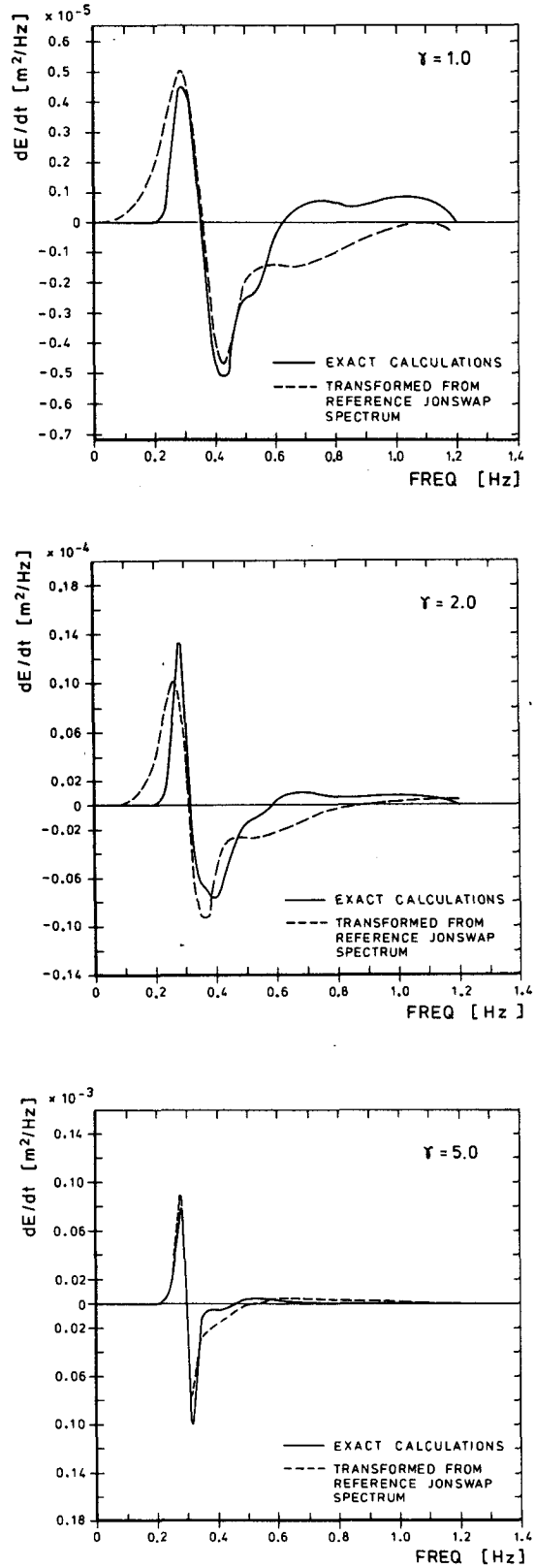

FIG. 3. Comparison of exact computations of one-dimensional S_{nl} distributions for JONSWAP spectra with $\gamma = 1$, 2 and 5 with parameterized form obtained by transforming from standard JONSWAP spectrum ($\gamma = 3.3$).

is to represent the set of computed functions $S_{nl}(f, \varphi)$ in a suitably chosen finite-dimensional function space. The most efficient function space for this purpose is the set of empirical orthogonal functions (EOFs) determined by the computed S_{nl} ensemble itself.

We have used this technique to parameterize S_{nl} in terms of two shape parameters, the peak-enhancement factor γ and a directional spread parameter s defined as the rms angular width of the spectrum,

$$s = [\overline{\Delta\varphi^2}]^{1/2} = \left[\int\int F(f, \varphi)(\varphi - \bar{\varphi})^2 df d\varphi/\epsilon\right]^{1/2} \quad (3.1)$$

where $\bar{\varphi} = \arctan(\overline{\sin\varphi}/\overline{\cos\varphi})$ denotes the (spectrally averaged) mean propagation direction.

The dependence of S_{nl} on γ and s was inferred from a set of 18 exact computations for various JONSWAP type spectral distributions with γ values varying from 1 to 7 and a number of different spreading functions (cf. Hasselmann and Hasselmann, 1981).

The ensemble of computed functions $S^{\alpha}_{nl}(f, \varphi)$, $\alpha = 1, \cdots 18$, were normalized through the energy ϵ and f_m in accordance with the scaling relation I, (3.3) and then expanded in terms of the mean source function

$$\bar{S}_{nl} = \frac{1}{18}\sum_{\alpha=1}^{18} S^{\alpha}_{nl}$$

and the set of EOF functions H^{β}_{nl} describing the variability of the ensemble relative to the mean,

$$S^{\alpha}_{nl} = \bar{S}_{nl} + \sum_{\beta=1}^{5} C^{\alpha\beta} H^{\beta}_{nl} \quad \alpha = 1, \cdots 18. \quad (3.2)$$

The expansion was terminated after the fifth EOF, as the higher EOFs could not be distinguished from noise in accordance with the criteria of Preisendorfer and Barnett (1977).

The ensemble of expansion coefficients $C^{\alpha\beta}$ was used to infer the dependence of the coefficients on the shape parameters γ and s, which was represented by a polynomial fit in the range $1 \leqslant \gamma \leqslant 3.3$ and $0.444 \leqslant s \leqslant 0.699$.

The source function for an arbitrary spectrum was thus finally expressed in the form

$$S_{nl}(\nu, \varphi) = \frac{a\epsilon^3 f_m^8}{g^4}\left[\bar{S}_{nl}(\nu, \varphi) + \sum_{\beta=1}^{5} C^{\beta}(\gamma, s) H^{\beta}_{nl}(\nu, \varphi)\right]. \quad (3.3)$$

In an operational model, the five functions H^{β}_{nl} and coefficients C^{β} are stored in memory, and Eq. (3.3) then provides a simple and computationally rapid estimate of S_{nl}. The technique has been applied in the model DNS by Allender *et al.* (1985).

A comparison of the parametrical approximations and exact computations of $S_{nl}(f, \varphi)$ are shown for a Pierson-Moskowitz spectrum ($\gamma = 1$) and JONSWAP spectrum ($\gamma = 3.3$) and different types of spreading functions in Fig. 4. The estimation of S_{nl} for the PM spectrum of Fig. 4a is excellent, as expected since this case (JONSWAP spectrum with a $\cos^2\varphi$ spreading function) was one of the 18 used in the construction of (3.3). The second comparison, Fig. 4b, however, represents a test of (3.3) for a 2d-spectrum with a spreading function of the form (2.4), which was not in the original set of 18.

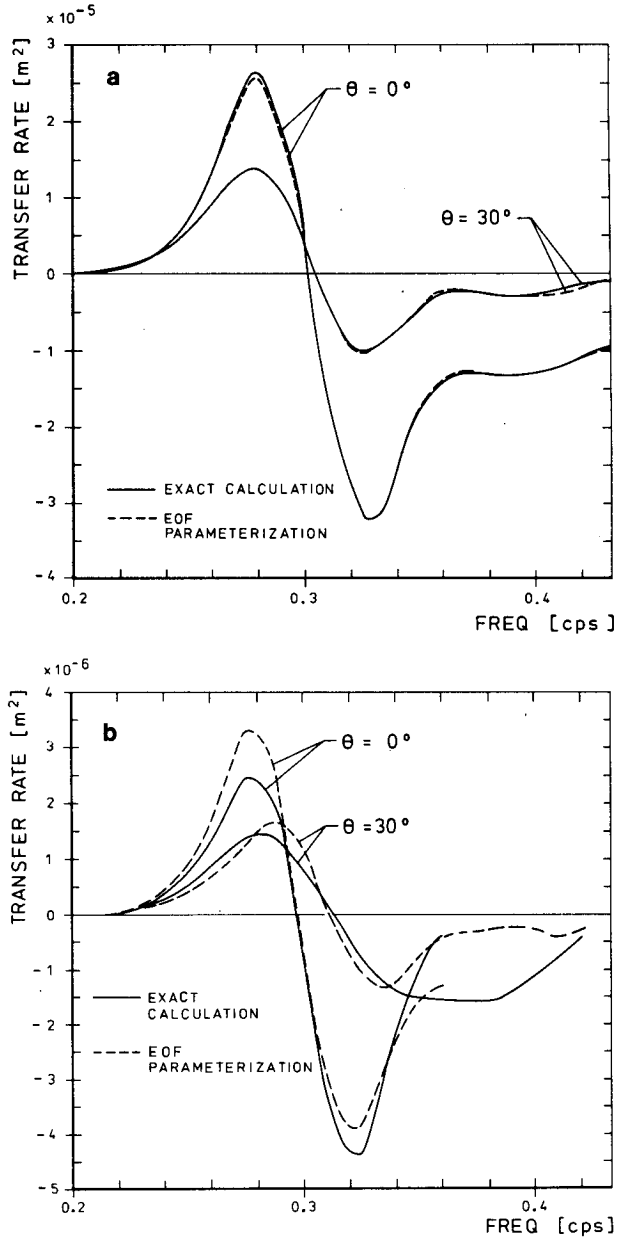

FIG. 4. Comparison of exact computations of the two-dimensional functions S_{nl} with the parameterized form derived from an EOF expansion. Case (a) ($\cos^2\theta$ spreading function) represents a member of the ensemble of cases used to construct the EOFs (thus the agreement is necessarily good), while case (b) corresponds to a spreading function of the form (4.4) which was not a member of the ensemble. The one-dimensional spectra are JONSWAP spectra in both cases.

4. Diffusion operator (local interaction) approximation

Both parameterization techniques described in the previous two sections are limited to a relatively restricted class of spectra which can be characterized by one or two shape parameters. The methods can clearly be extended to more parameters. However, it appears questionable whether this is a profitable route to pursue, for the methods also suffer from a more basic shortcoming: as pointed out above, they lead generally to instabilities when applied in discrete wave models in which the spectral representations contain more degrees of freedom than used in the parameterization of the nonlinear transfer. This is a consequence of the role played by the nonlinear transfer in establishing a balance between the different distributions of the input and dissipation source functions. The balance involves a delicate adjustment of the spectral shape and the associated nonlinear transfer (cf. Komen *et al.*, 1984), which cannot be achieved if the parameterization of S_{nl} has too few degrees of freedom to generate the required spectral form. The unavoidable residual imbalance of the net source function leads to unstable growth of the spectrum in those degrees of freedom which cannot be compensated by the parameterized nonlinear transfer.

In existing wave models this problem is resolved by restricting the form of the spectrum in the unstable regimes. This effectively reduces a potentially fully resolving discrete spectral model to a hybrid-type model (cf. The SWAMP Group, 1985). A more appropriate solution to the problem is clearly to devise parameterizations based on the same number of degrees of freedom as used in the representation of the spectrum, i.e., to develop operator parameterizations.

Boltzmann integrals of the form of the nonlinear transfer expression [I, Eq. (2.1)] are often approximated by a differential-operator expression derived from a local-interaction expansion. In the case of a wave field scattered by a given external field, this yields the well-known linear second-order Fokker-Planck diffusion operator for small angle scattering. In the present case of third-order interactions between components of the same wave field, the local interaction expansion yields a cubic, fourth-order diffusion operator of the general form (cf. Hasselmann and Hasselmann, 1981)

$$\frac{d}{dt}n = \frac{\partial^2}{\partial k_i \partial k_j}\left(D_{ijmn}\left[n^2\frac{\partial^2}{\partial k_m \partial k_n} - 2n\frac{\partial n}{\partial k_m}\frac{\partial n}{\partial k_n}\right]\right) \tag{4.1}$$

where the coefficients are given by

$$D_{ijmn} = 2^{-10}\iint \sigma\cdot\delta(\omega_1+\omega_2-\omega_3-\omega_4) \times (k'_m k'_n - k''_m k''_n)(k'_i k'_j - k''_i k''_j)d\mathbf{k}'d\mathbf{k}'' \tag{4.2}$$

with

$$\mathbf{k}_1 = \frac{\mathbf{k}+\mathbf{k}'}{2},\quad \mathbf{k}_2 = \frac{\mathbf{k}-\mathbf{k}'}{2},\qquad \mathbf{k}_3 = \frac{\mathbf{k}+\mathbf{k}''}{2},\quad \mathbf{k}_4 = \frac{\mathbf{k}-\mathbf{k}''}{2}. \tag{4.3}$$

For deep-water waves, $D_{ijmn} \sim g^{3/2}k^{27/2}$ and the general tensor form (4.1) can be reduced by applying conservation and symmetry considerations to a form containing only two scalar numerical coefficients C_1, C_2,

$$\frac{dn}{dt} = C_1\cdot\left(\nabla^2 + \frac{\partial^2}{\partial k_i\partial k_j}\frac{k_i k_j}{k^2}\right)(A+D) + C_2\cdot\left\{\left(2\cdot\frac{\partial^2}{\partial k_i\partial k_j}\frac{k_i k_j}{k^2}\right)A + \frac{\partial^2}{\partial k_i\partial k_j}B_{ij} + \left(2\nabla^2 - \frac{\partial^2}{\partial k_i\partial k_j}\frac{k_i k_j}{k^2}\right)D\right\} \tag{4.4}$$

where

$$A = g^{3/2}k^{27/2}\left(n^2\frac{\partial^2 n}{\partial k_m\partial k_m} - 2n\frac{\partial n}{\partial k_m}\cdot\frac{\partial n}{\partial k_m}\right)$$

$$B_{ij} = g^{3/2}k^{27/2}\left(n^2\frac{\partial^2 n}{\partial k_i\partial k_j} - 2n\frac{\partial n}{\partial k_i}\frac{\partial n}{\partial k_j}\right)$$

$$D = g^{3/2}k^{27/2}\left\{\frac{k_m k_n}{k^2}\left(n^2\frac{\partial^2 n}{\partial k_m\partial k_n} - 2n\frac{\partial n}{\partial k_m}\cdot\frac{\partial n}{\partial k_n}\right)\right\}.$$

Details are given by Hasselmann and Hasselmann (1981).

The local-interaction approximation is appropriate if the principal interactions occur in the vicinity of the central interaction point $\mathbf{k}_1 = \mathbf{k}_2 = \mathbf{k}_3 = \mathbf{k}_4 = \hat{\mathbf{k}}$ in which all wavenumbers of the interacting quadruplet are the same. It is found that the scattering coefficient σ does indeed have a maximum at this point (cf. Hasselmann, 1963), and this region in interaction phase space is furthermore strongly weighted through a stationarity in the argument of the frequency δ-function. The approximation is suggested also by the exact nonlinear transfer computations, which exhibit various short-range features typical of a local diffusion-operator expression (cf. I, Section 5).

A comparison of an optimally fitted diffusion-operator expression of the specific form

$$\left(\frac{dn}{dt}\right)_{nl} = 0.019\cdot g^{3/2}\left\{\left[\frac{\partial^2}{\partial k_i\partial k_i} + \frac{\partial^2}{\partial k_i\partial k_j}\frac{k_i k_j}{k^2}\right]k^{27/2} \times\left[n^2\frac{\partial^2 n}{\partial k_m\partial k_m} - 2n\frac{\partial n}{\partial k_m}\frac{\partial n}{\partial k_m} + \frac{k_m k_n}{k^2} \times\left(n^2\frac{\partial^2 n}{\partial k_m\partial k_n} - 2n\frac{\partial n}{\partial k_m}\frac{\partial n}{\partial k_n}\right)\right]\right\} \tag{4.5}$$

with exact computations is given in Fig. 5a, b. Although

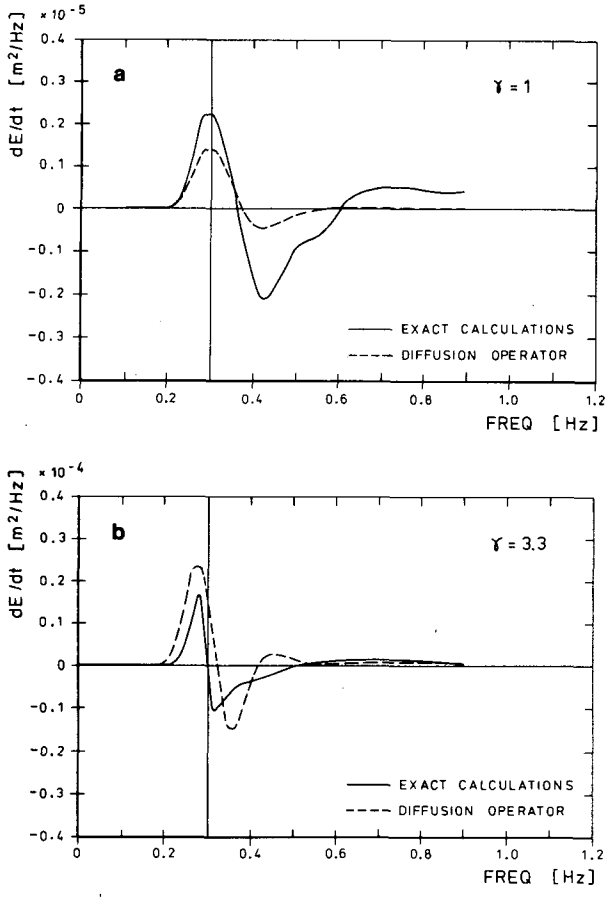

FIG. 5. Comparison of the exact one-dimensional distributions S_{nl} with the local-interaction approximation for a Pierson-Moskowitz spectrum (panel a) and a JONSWAP spectrum (panel b).

the diffusion operator clearly captures the qualitative features of the exact expression fairly well, it was found to be impossible to tune expressions of the form (4.4) to reproduce the source functions S_{nl} for both growing and fully developed wind seas quantitatively. In particular, the transfer rate for the Pierson-Moskowitz spectrum is seen to be too low by a factor of two relative to the JONSWAP case. Investigations of the contributions to the exact transfer integral from different regions of the interaction phase space (I, Section 5) confirm that the diffusion operator does indeed provide a good approximation to the contributions in the neighbourhood of the central interaction point, but contributions from more distant regions of the interaction phase space cannot be neglected, particularly for the less highly peaked Pierson-Moskowitz spectrum. In fact, the principal contributions to the nonlinear transfer come from intermediate wavenumber quadruplets whose separations are probably slightly too large to be adequately represented by a local interaction expansion.

Experiments were also made with various simpler, second-order, cubic diffusion operators, with results which were qualitatively similar to the fourth-order expression, and exhibited the same limitations.

The narrow-peak approximations of Longuet-Higgins (1976), Fox (1976) and Dungey and Hui (1979) also consider interactions only in the neighborhood of the central interaction point. The narrow-peak and local-interaction approximations are nevertheless based on different assumptions. In the diffusion-operator approximation it is assumed that the spectrum is smooth and the scattering coefficient is strongly peaked, whereas these requirements are interchanged for the narrow-peak approximation. Both approximations, however, apply the same expansions of the resonance δ-functions, which weight the central interaction region by the singularity at the stationary center point. The local-interaction approximation is more general in the sense that it applies for arbitrary spectra, provided they are not too extremely peaked, and for all regions of the spectrum, including regions far removed from the peak.

Although not sufficiently accurate for use in most wave models, the nonlinear diffusion-operator approximation is helpful for understanding the mechanism by which the nonlinear transfer generates and maintains the shape of the spectrum. Intuitively, one would expect the nonlinear redistribution of energy to smooth out the spectrum, rather than produce a sharp spectral peak with a steep forward face. This is true generally for linear diffusion operators. However, the nonlinearity, together with the strong wavenumber dependence, of the diffusion operator produces a strong inhomogeneity of the diffusive energy (or action) flux, which results in the generation of frontal-type structures in wavenumber space. The fluxes are high in regions of high energy and high wavenumbers, and low in regions of low energy and low wavenumbers. Hence a strong energy flux convergence occurs in the transition region between the peak of the spectrum and the very low-energy region at slightly lower wavenumbers. The convergence causes the front on the forward face of the spectrum to steepen, and to migrate towards lower wavenumbers, as energy is continually fed into the front from the high-energy, high-wavenumber side. The front finally decays when it runs beyond the wavenumber region in which the spectrum receives energy from the wind, and the energy supply to the front is cut off.

5. The discrete interaction approximation

Since the interactions between closely neighboring wavenumbers already reproduce the principal features of the nonlinear transfer, it appears fruitful to explore alternative parameterizations that bear some similarity to the local-interaction approximation but are able to overcome the shortcomings of this approach. To this end we considered a nonlinear interaction operator constructed by the superposition of a small number of discrete-interaction configurations composed of neighboring and finite-distance interaction combi-

nations. After some experimentation it was found that the exact nonlinear transfer could in fact be well simulated by just one mirror-image pair of intermediate-range interaction configurations.

In each configuration, two wavenumbers were taken as identical, $\mathbf{k}_1 = \mathbf{k}_2 \equiv \mathbf{k}$. The wavenumbers $\mathbf{k}_3$ and $\mathbf{k}_4$ are of different magnitude and lie at an angle to the wavenumber $\mathbf{k}$, as required by the resonance conditions. The second configuration is obtained from the first by reflecting the wavenumbers $\mathbf{k}_3$ and $\mathbf{k}_4$ at the $\mathbf{k}$-axis (cf. Fig. 6). The scale and direction of the reference wavenumber $\mathbf{k}$ are allowed to vary continuously in the wavenumber plane.

The reduced nonlinear operator is computed by applying the same symmetrical interaction phase-space integration method as used to compute the exact transfer integral (cf. I). The interactions are summed over the (discretized) $\mathbf{k}$-plane and, for each $\mathbf{k}$, over the pair of discrete-interaction configurations. For each interaction ("collision") the changes in action ("particle number") for all four interacting wavenumbers are stored in the appropriate bins of the two-dimensional source-function array $S_{nl}(f, \varphi)$. The computation is identical to the computation of the exact Boltzmann integral except that the integration is taken over a 2d-continuum and two discrete interactions instead of a 5d-interaction phase space. As in the exact case, the interactions conserve energy, momentum and action.

Satisfactory agreement with the exact computations was obtained with the configuration

$$\omega_1 = \omega_2 = \omega \tag{5.1}$$

$$\omega_3 = \omega(1 + \lambda) = \omega_+ \tag{5.2}$$

$$\omega_4 = \omega(1 - \lambda) = \omega_- \tag{5.3}$$

with $\lambda = 0.25$. From the resonance conditions the angles θ_3, θ_4 of the wavenumbers $\mathbf{k}_3(\mathbf{k}_+)$ and $\mathbf{k}_4(\mathbf{k}_-)$ relative to $\mathbf{k}$ are found to be $\theta_3 = 11.5°$, $\theta_4 = -33.6°$.

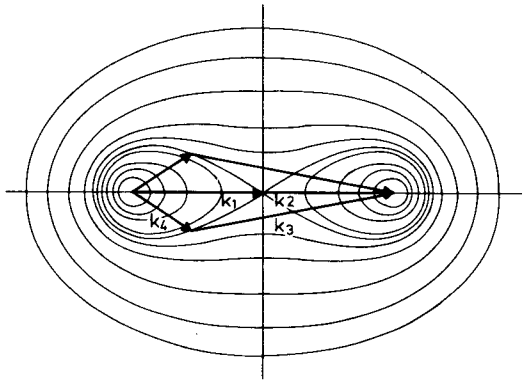

FIG. 6. The two interaction configurations used in the discrete-interaction approximation. Contour lines represent the possible end points of the vectors $\mathbf{k}_1$ and $\mathbf{k}_4$ for any interaction quadruplet in the full interaction space (cf. Hasselmann, 1962).

The appropriate discrete-interaction analogue to the exact symmetrical interaction expressions [I, Eqs. (2.1)–(2.6)] is given by

$$\begin{Bmatrix} \delta n \\ \delta n_+ \\ \delta n_- \end{Bmatrix} = \begin{Bmatrix} -2 \\ 1 \\ 1 \end{Bmatrix} C' g^{-8} f^{19} \times [n^2(n_+ + n_-) - 2nn_+n_-]\Delta\mathbf{k}\Delta t \tag{5.4}$$

where δn, δn_+, δn_- represent the increments in action ("particle number") occurring in the time Δt at the interacting wavenumbers $\mathbf{k}$, $\mathbf{k}_+$, $\mathbf{k}_-$ due to the discrete interactions ('particle collision') within the infinitesimal interaction phase–space element $\Delta\mathbf{k}$, and C' is a numerical constant representing the strength of the interaction.

In practice, Eq. (5.4) normally needs to be translated into changes in the energy spectral densities F with respect to frequency f and propagation direction φ, and for the interaction phase-space variables it is then similarly more convenient to use f and φ rather than $\mathbf{k}$. In terms of these variables, one obtains for the increments to the source functions $S_{nl}(f, \varphi)$ at the three interacting wavenumbers (frequencies and directions)

$$\begin{Bmatrix} \delta S_{nl} \\ \delta S^+_{nl} \\ \delta S^-_{nl} \end{Bmatrix} = \begin{Bmatrix} -2\dfrac{\Delta f\Delta\varphi}{\Delta f\Delta\varphi} \\ (1+\lambda)\dfrac{\Delta f\Delta\varphi}{\Delta f^+\Delta\varphi} \\ (1-\lambda)\dfrac{\Delta f\Delta\varphi}{\Delta f^-\Delta\varphi} \end{Bmatrix} \times Cg^{-4}f^{11}\left[F^2\left(\frac{F_+}{(1+\lambda)^4} + \frac{F_-}{(1-\lambda)^4}\right) - 2\frac{FF_+F_-}{(1-\lambda^2)^4}\right] \tag{5.5}$$

where C is a modified numerical constant proportional to C' and Δf, Δf^+, Δf^- denote the discrete resolution of the spectrum and source function at the frequencies f, f^+, f^-, respectively. The increments $\Delta f\Delta\varphi$ in the numerator refer here to the discrete-interaction phase–space element, while the differentials in the denominator refer to the sizes of the "bins" in which the incremental spectral changes induced by a "collision" are stored. For simplicity, we have taken both angular increments $\Delta\varphi$ to be the same, but have allowed for a possible frequency dependence of Δf, in which case $\Delta f^+ \neq \Delta f^- \neq \Delta f$.

Equation (5.5) is summed over all frequencies, directions and interaction configurations to yield the net source function S_{nl}.

A comparison of the approximate and exact transfer source function for a JONSWAP spectrum is shown in Fig. 7. The coefficient C in Eq. (5.5) was chosen as

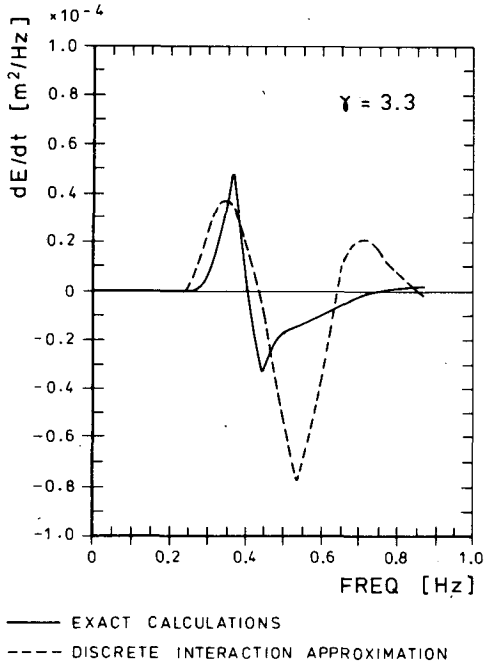

FIG. 7. Comparison of the exact one-dimensional distribution S_{nl} with the discrete-interaction approximation for a JONSWAP spectrum.

3×10^7. The distributions agree reasonably well, except for the relatively strong negative lobe of the discrete interaction approximation. However, this feature is less important for a satisfactory reproduction of wave growth than the correctly simulated form of the positive lobe, which controls the rate at which the spectral peak shifts towards lower frequencies.

Figure 8 shows a comparison of the fetch-limited growth curves for some characteristic spectral parameters computed with a wave model using the exact nonlinear transfer expression or, alternatively, the discrete-interaction approximation. The corresponding one-dimensional spectra are shown in Fig. 9. The effect of the stronger negative lobe of the discrete-interaction parameterization is evidenced by the 10–15% smaller values of α. The somewhat smaller values of γ for the parameterized case seen in Fig. 8 (top right panel) are also apparent in Fig. 9. However, the agreement of the more important scale parameters, the energy E^* and peak frequency f_m^*, is excellent. (An asterisk denotes nondimensionalization of a variable through g and the friction velocity u_*.)

The remaining source functions used in the model integrations are taken from the study on growing and fully developed wind fields by Komen *et al.* (1984).

The input source function is given by

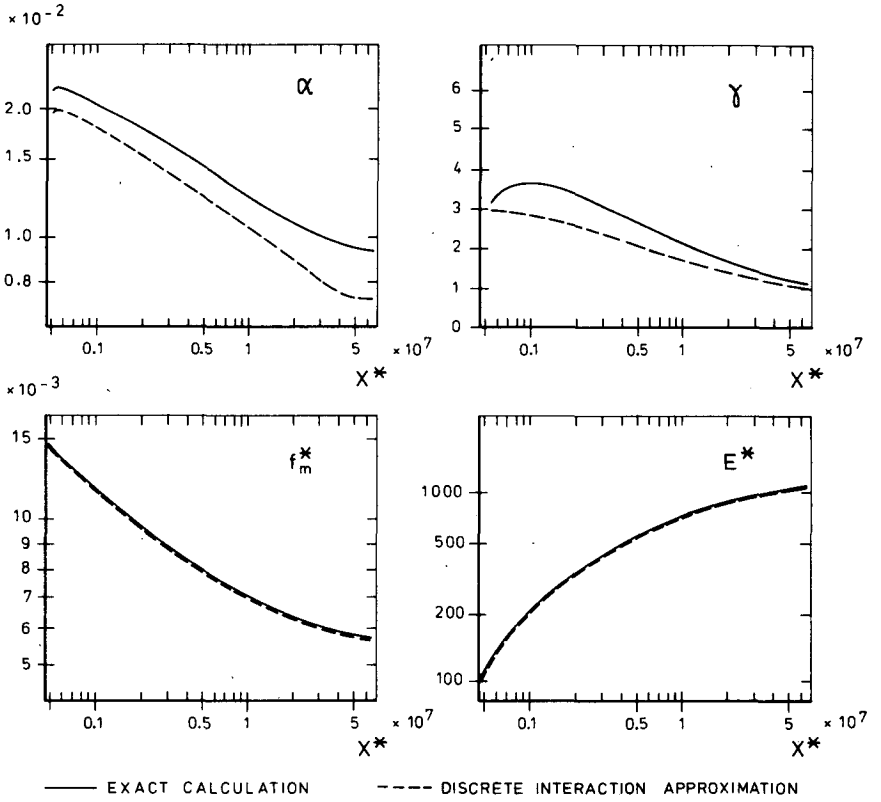

FIG. 8. Comparison of the fetch-growth curves for spectral parameters computed using the exact form and the discrete-interaction approximation of S_{nl}. All variables are made dimensionless using u_* and g.

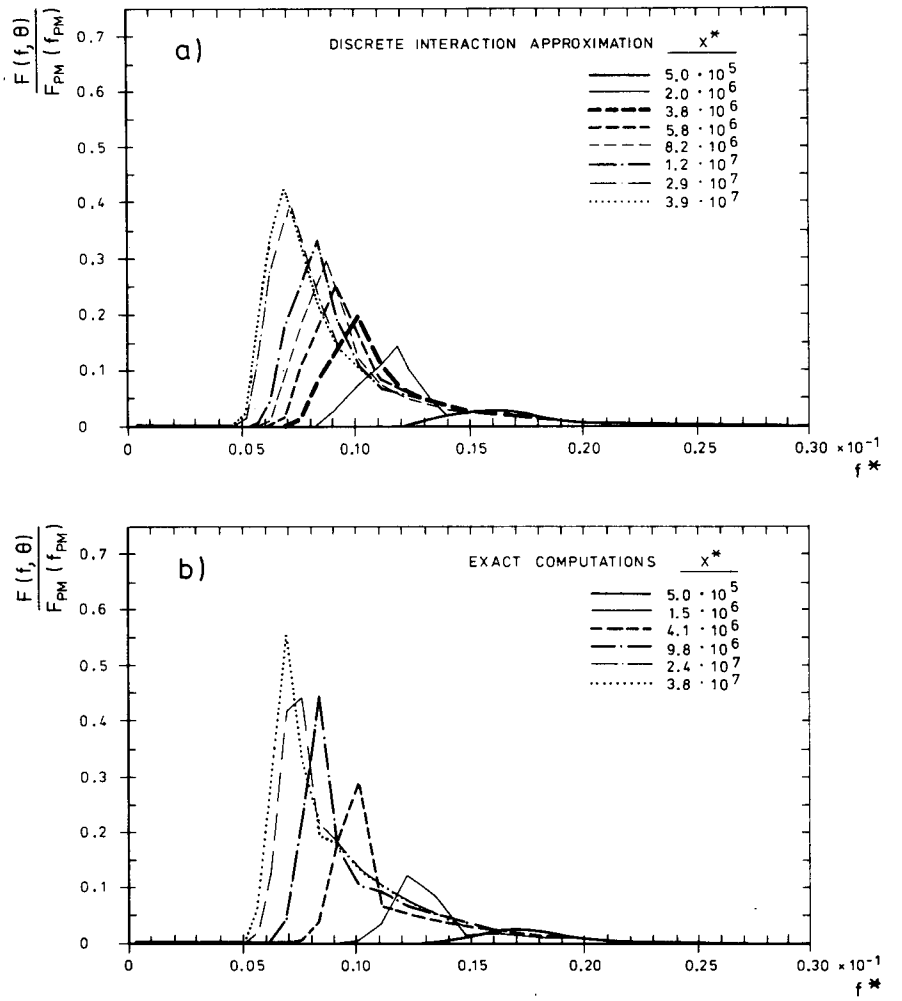

FIG. 9. Comparison of the growth of fetch-limited one-dimensional spectra computed using the discrete-interaction approximation (panel a) and the exact form of S_{nl} (panel b).

$$S_{in}(f,\theta) = \max\left[0., 0.25\,\frac{\rho_a}{\rho_w} \times \left(\frac{28u_*}{c}\cos\theta - 1\right)\cdot \omega F(f,\theta)\right]$$

following Snyder *et al.* (1981), but with the replacement of their wind-speed U_5 dependence by a similar dependence on the friction velocity $u_* = U_5/28$.

The dissipation source function is given by

$$S_{ds}(f,\theta) = -1.6\bar{\omega}(\omega/\bar{\omega})^2\hat{\alpha}^2\cdot F(f,\theta)$$

with

$$\hat{\alpha} = \epsilon\cdot\bar{\omega}^4/g^2$$

$$\bar{\omega} = \epsilon^{-1}\int F(f,\theta)\cdot\omega\,df\,d\theta$$

following Hasselmann's (1974) general form for the dissipation due to small-scale whitecapping processes.

In general, it was found that the most critical test of a parameterization of S_{nl} was its ability to reproduce the correct wave growth, rather than a superficial visual agreement of transfer-function computations for individual spectra. This is borne out by a comparison of the energy balance for the exact and discrete interaction cases at small fetch (Fig. 10) and near full development (Fig. 11). The agreement of the spectra and energy balance is closer than may have been anticipated from Fig. 7. The explanation is that the spectrum adjusts slightly in shape to the slightly incorrect form of the nonlinear transfer. If the tuning is then carried out such that the growth curves are approximately correct for the adjusted spectrum (rather than by trying to reproduce the nonlinear transfer for a prescribed theoretical spectrum, as in Fig. 7), the resulting energy balance is also simulated rather accurately.

The principal motivation for retaining the general operator character of the exact Boltzmann integral in the parameterization of S_{nl} was to be able to represent the nonlinear transfer for arbitrary spectral distributions, in order to develop third-generation wave models

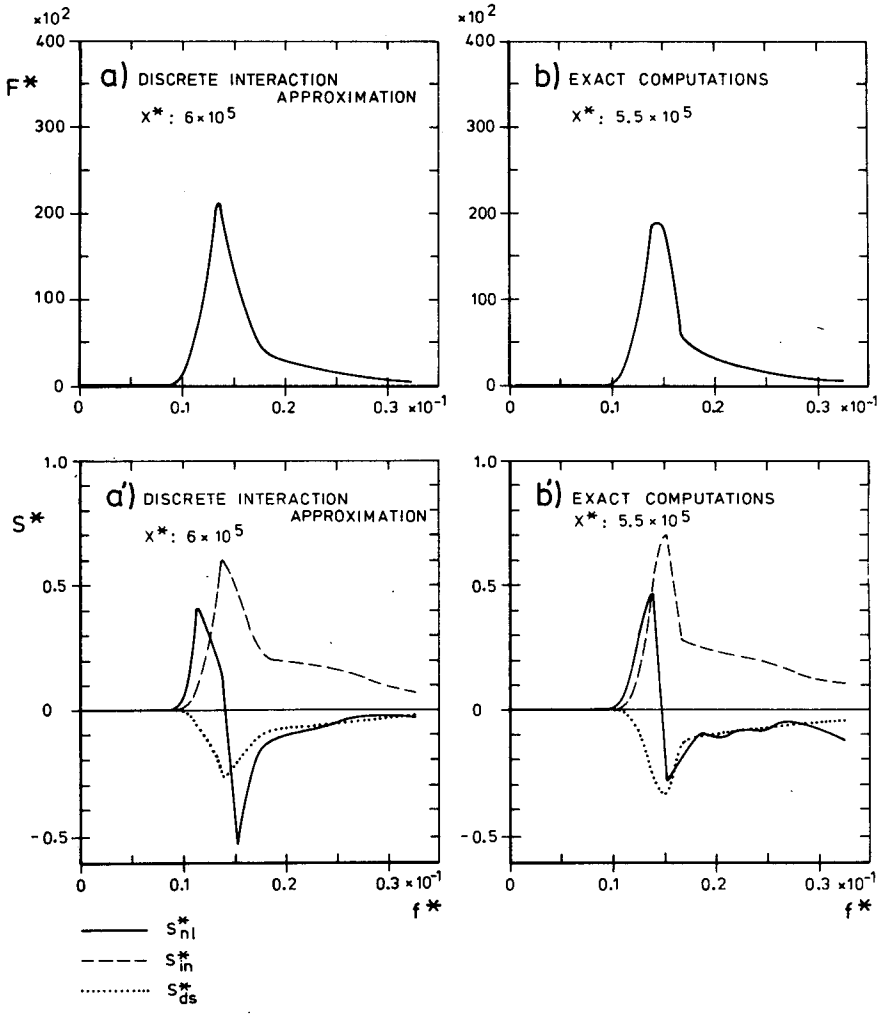

FIG. 10. Spectral and energy balance of fetch-limited spectra at small fetch ($x^* \approx 6 \times 10^5$) computed using the discrete-interaction approximation (panels a, a') and exact computation of S_{nl} (panels b, b').

based solely on the energy balance equation, free from additional restraints regarding the spectral shape. It is therefore important to note that the simulation of the observed wave growth in Figs. 8 and 9, including the continuous transition from a fetch-limited to a fully developed wind-sea spectrum, was achieved without any prior assumptions regarding the shape of the spectrum.

An independent test of the general applicability of the discrete-interaction approximation is provided by the response of a wind sea to a sudden, 90° shift in wind direction (SWAMP, case 7, The SWAMP Group, 1985). The discrete-interaction approximation is seen to reproduce the main features of the exact integration rather well (Fig. 12).

A more extensive set of tests on the response of a wind-sea spectrum to turning winds has been carried out by Young *et al.* (1985). Good agreement between the exact computations and the discrete-interaction approximation was found also in these cases.

The discrete-interaction parameterization is currently being incorporated in a third-generation global discrete spectral wave model in development in Hamburg, in collaboration with the Wave Modelling (WAM) Group. The method can be readily upgraded by including further discrete-interaction configurations. It can be applied also to finite-depth water waves by introducing a depth dependence into the coefficients C of Eq. (5.5) and (if necessary) in the angles of the interacting wave components $\mathbf{k}_3$, $\mathbf{k}_4$.

6. Conclusions

The principal motivation for developing new parameterizations of S_{nl} is a basic shortcoming of the parameterizations used in existing second-generation wave models: the parameterizations are unable to reproduce the observed form of a growing wind-sea spectrum if introduced without *ad hoc* constraints into a fully resolving spectral model. The problem lies in the

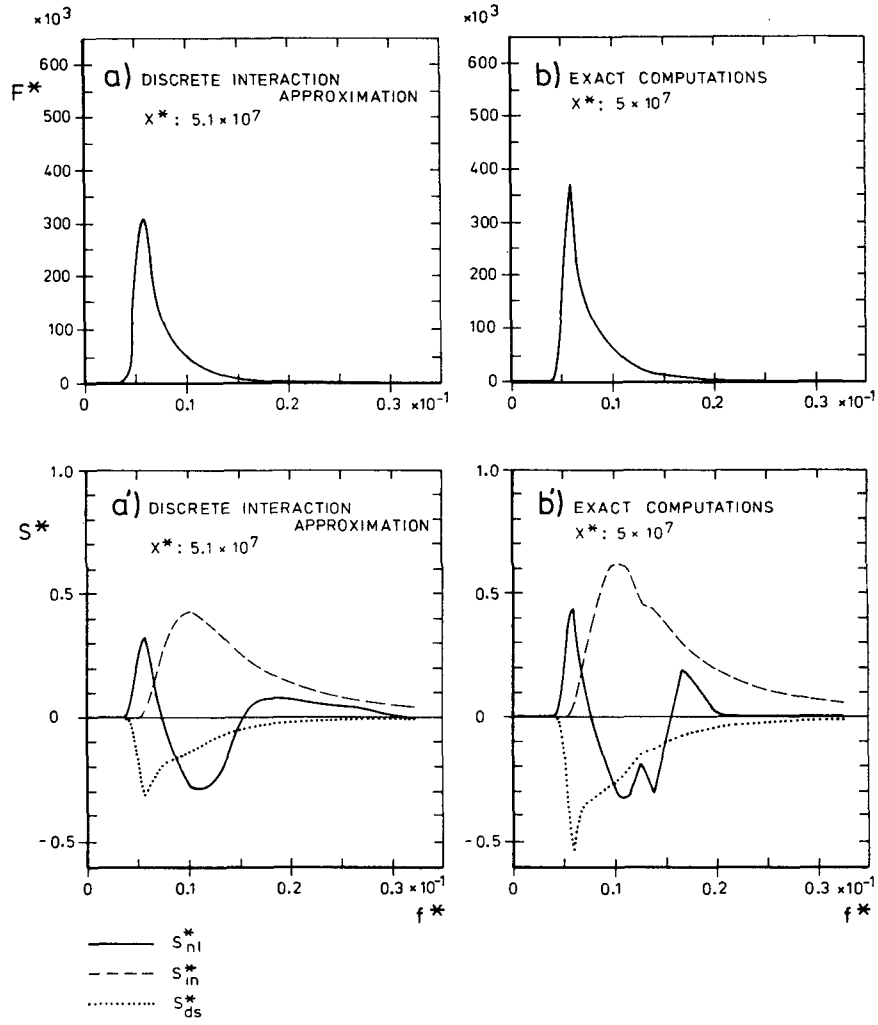

FIG. 11. As in Fig. 10 for nearly fully developed specta ($x^* \approx 5 \times 10^7$).

approximate representation of S_{nl} in terms of relatively few freely adjustable parameters. This does not provide the flexibility needed for the nonlinear transfer to be able to adjust the spectrum to the shape required for S_{nl} to balance the input and dissipation source functions in the quasi-equilibrium range of the spectrum, giving rise to instabilities.

The problem is resolved in present discrete wave models by effectively restricting the form of the wind-sea spectrum. However, this eliminates the potential advantage of a discrete wave model over a simpler parametrical model in which the spectral shape is restricted already in the basic formulation of the model. Consequently, both discrete and parametrical second-generation models suffer from the same basic difficulties in modeling wind-sea spectra which do not conform to the standard JONSWAP type quasi-equilibrium distribution, as encountered, for example, in rapidly changing wind fields or in slanting fetch situations. Both classes of model are similarly unable to treat the wind sea–swell transition regime, which is also characterized by a wide variety of possible spectral distributions, without introducing *ad hoc* empirical assumptions.

These limitations can be overcome only by introducing operator parameterizations of S_{nl} that contain the same number of degrees of freedom as used to describe the spectrum, and that can be applied to arbitrary spectra. After considering other parameterizations, we propose a discrete-interaction operator parameterization that is structured in the same way as the exact Boltzmann-integral expression but is based on only two elementary interaction configurations. The discrete-interaction parameterization has been tested and tuned against a number of model integrations using the exact form of S_{nl}. It can readily be improved, if found desirable through further experience, by inclusion of additional interaction configurations.

Although less relevant for application in third-generation, discrete spectral models, the three other parameterizations considered in this paper also exhibited certain useful features.

The simple distortion transformation, applied to the

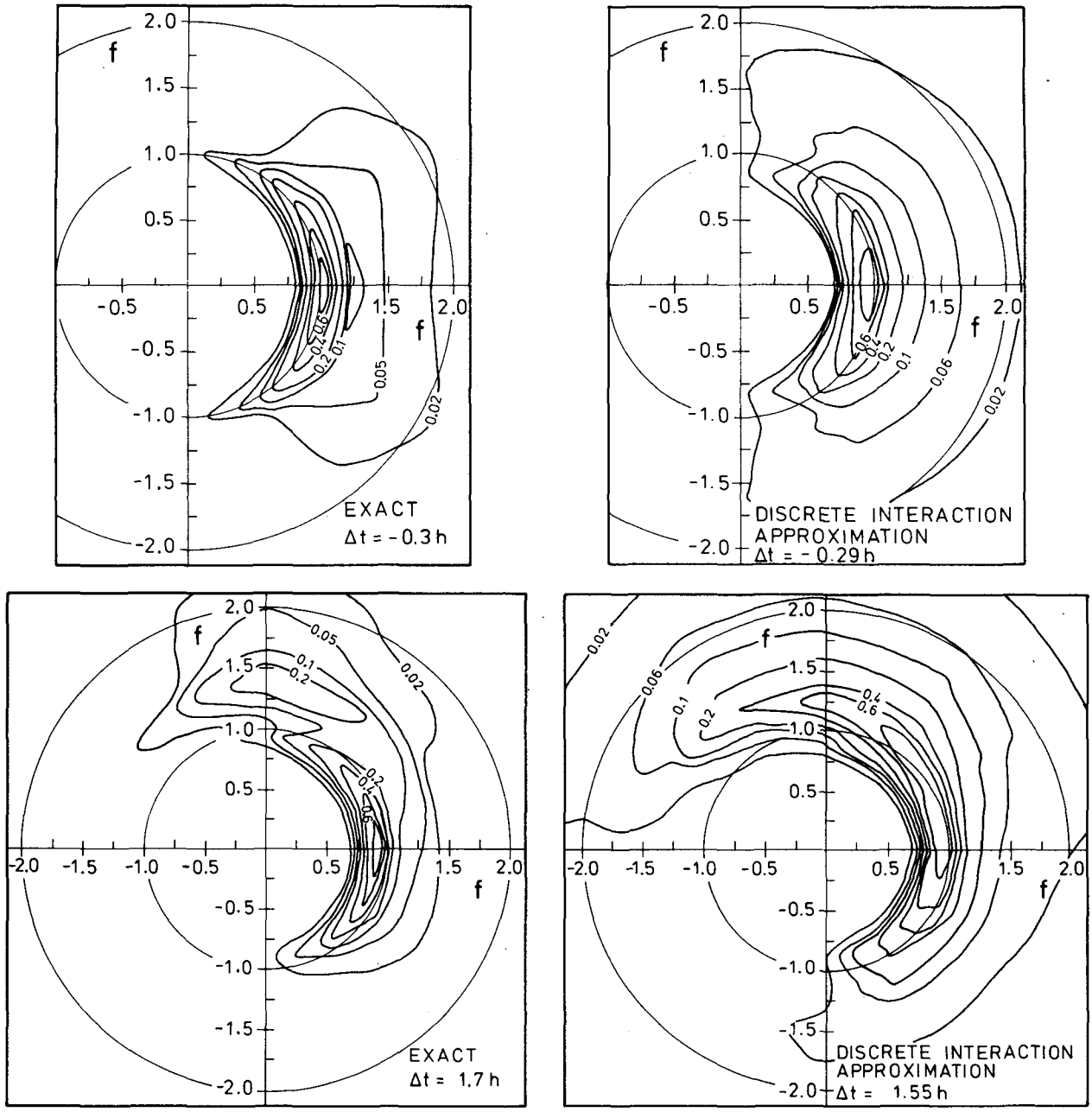

FIG. 12. Comparison of the response of a two-dimensional wave spectrum to a sudden 90° change in wind direction at time t_0 computed using the exact form and the discrete-interaction approximation of S_{nl}. $\Delta t = t - t_0$, and t_0 is the time at which the peak frequency is just twice the fully developed peak frequency. The strength of the wind forcing remains constant ($u_* = 0.357$ m s^{-1}).

reference source function S_{nl}^{ref} for a standard JONSWAP spectrum, provides a convenient description of the modification of S_{nl} occurring during the development of a wind-sea spectrum. The plotted variations of the transformation coefficients with γ summarize these changes concisely and can be used for calculating the magnitude and form of the source function S_{nl} for different stages of wave growth.

The parameterizations of S_{nl} in terms of an EOF expansion is of interest, as it has been incorporated in an existing discrete spectral wave model (Allender *et al.*, 1985) and allows a moderate degree of adjustment of the spectral shape near the peak and on the forward face of the spectrum (although the quasi-equilibrium range of the spectrum still has to be specified, as in other second generation models).

The parameterization in terms of a cubic, fourth-order diffusion operator, finally, has the advantage that it is derived by a well defined expansion procedure for small scattering angles, retains the principal features

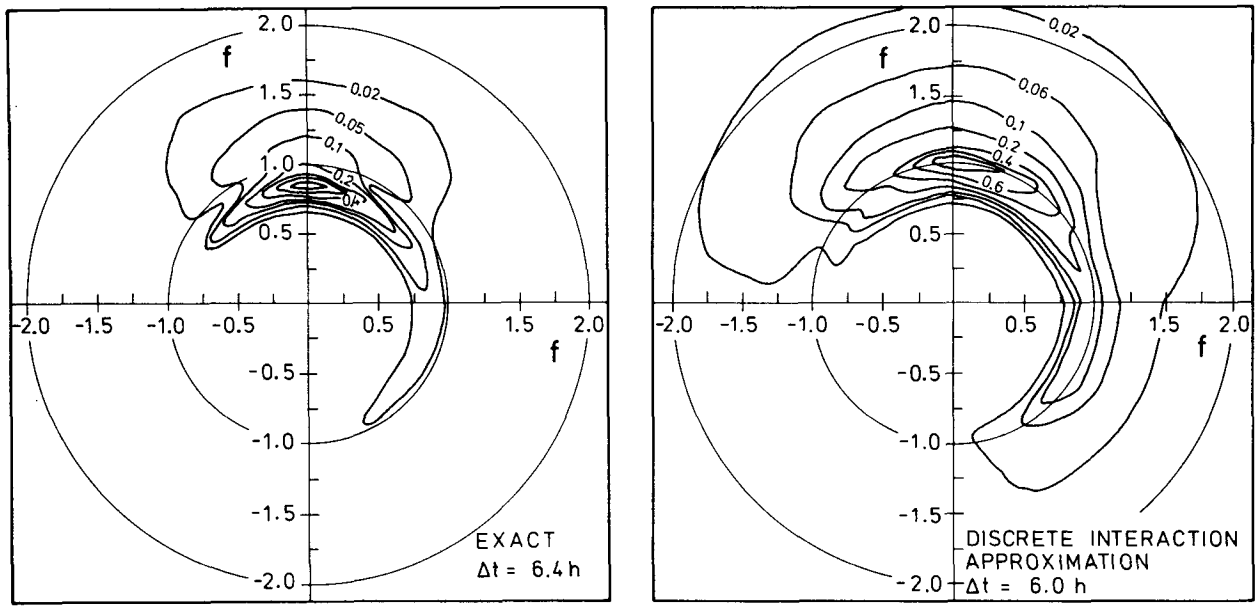

FIG. 12. (*Continued*)

of the complete expression and can be used to explain certain basic properties of the nonlinear transfer, such as the generation of a self-stabilizing, highly peaked spectral shape with a frontal structure on the forward face, which are difficult to deduce from the complete Boltzmann integral or the discrete interaction approximation.

Acknowledgments. This work was partly supported by the Office of Naval Research under Contracts N00014-77-9-0054 and N000-14-80-C-0440/OMNIBUS and the European Space Agency under Contract 5544/83/F/CG.

REFERENCES

Allender, J. H., T. P. Barnett and M. Lybanon, 1985: An improved spectral model for ocean wave prediction. *Ocean Wave Modeling,* The SWAMP Group, Plenum, 256 pp.

Barnett, T. P., 1968: On the generation, dissipation and prediction of ocean wind waves. *J. Geophys. Res.,* **73,** 513–530.

Dungey, J. C., and W. H. Hui, 1979: Nonlinear energy transfer in a narrow gravity-wave spectrum. *Proc. Roy. Soc. London,* **A368,** 239–265.

Ewing, J. A., 1971: A numerical wave prediction method for the North Atlantic Ocean. *Dtsch. Hydrogr. Z.,* **24,** 241–261.

Fox, M. J. H., 1976: On the nonlinear transfer of energy in the peak of a gravity-wave spectrum II. *Proc. Roy. Soc. London,* **A348,** 467–483.

Hasselmann, D. E., M. Dunckel and J. A. Ewing, 1980: Directional wave spectra observed during JONSWAP 1973. *J. Phys. Oceanogr.,* **10,** 1264–1280.

Hasselmann, K., 1962: On the nonlinear energy transfer in a gravity-wave spectrum. Part I: General theory. *J. Fluid Mech.,* **12,** 481–500.

——, 1963: On the nonlinear energy transfer in a gravity-wave spectrum. Part 3: Computation of the energy flux and swell-sea interaction for a Neumann spectrum. *J. Fluid Mech.,* **15,** 385–398.

——, 1974: On the spectral dissipation of ocean waves due to white capping. *Bound. Layer Meteor.,* **6,** 107–127.

——, and Collaborators, 1973: Measurements of wind-wave growth and swell decay during the Joint North Sea Wave Project (JONSWAP). *Dtsch. Hydrogr. Z.,* **A8,** 95 pp.

Hasselmann, S., and K. Hasselmann, 1981: A symmetrical method of computing the nonlinear transfer in a gravity-wave spectrum. *Hamb. Geophys. Einzelschriften, Reihe A: Wiss. Abhand.,* **52,** 138 pp.

——, and ——, 1985: Computations and parameterizations of the nonlinear energy transfer in a gravity wave spectrum. Part I: A new method for efficient computations of the exact nonlinear transfer integral. *J. Phys. Oceanogr.,* **15,** 1369–1377.

Komen, G. J., S. Hasselmann and K. Hasselmann, 1984: On the existence of a fully developed wind-sea spectrum. *J. Phys. Oceanogr.,* **14,** 1271–1285.

Longuet-Higgins, M. S., 1976: On the nonlinear transfer of energy in the peak of a gravity-wave spectrum. *Proc. Roy. Soc. London,* **A347,** 311–328.

Mitsuyasu, H., 1968: On the growth of the spectrum of wind-generated waves. 1. *Rep. Res. Inst. Appl. Mech., Kyushu Univ.,* **16,** 459–465.

——, 1969: On the growth on the spectrum of wind-generated waves. 2. *Rep. Res. Inst. Appl. Mech., Kyushu Univ.,* **17,** 235–243.

——, F. Tasai, T. Suhara, S. Mizuno, M. Ohkuso, T. Honda and K. Rikiishi, 1975: Observations of the directional spectrum of ocean waves using a clover leaf buoy. *J. Phys. Oceanogr.,* **5,** 750–760.

Preisendorfer, R. W., and T. P. Barnett, 1977: Significance test for empirical orthogonal functions. *Proc. Fifth Conf. on Probability and Statistics in Atmospheric Sciences,* Las Vegas, Amer. Meteor. Soc., 169–172.

Snyder, R. L., F. W. Dobson, J. A. Elliott and R. B. Long, 1981: Array measurements of atmospheric pressure fluctuations above surface gravity waves. *J. Fluid Mech.,* **102,** 1–59.

The SWAMP Group, 1985: Sea Wave Modelling Project (SWAMP). An intercomparison study of wind wave prediction models, Part 1: Principal results and conclusions. *Ocean Wave Modeling,* Plenum, 256 pp.

Young, I. R., S. Hasselmann and K. Hasselmann, 1985: Computations of the response of a wave spectrum to a sudden change in the wind direction, (in preparation).